

Low Frequency Switching in a Transistor Amplifier

T. L. Carroll

US Naval Research Lab, Washington, DC 20375

(January 31, 2003)

Abstract

It is known from extensive work with the diode resonator that the nonlinear properties of a PN junction can lead to period doubling, chaos, and other complicated behaviors in a driven circuit. There has been very little work on what happens when more than one PN junction is present. In this work, the first step towards multiple PN junction circuits is taken by doing both experiments and simulations with a single-transistor amplifier using a bipolar transistor. Period doubling and chaos are seen when the amplifier is driven with signals between 100 kHz and 1 MHz, and they coincide with a very low frequency switching between different period doubled (or chaotic) waveforms. The switching frequencies are between 5 and 10 Hz. The switching behavior was confirmed in a simplified model of the transistor amplifier.

05.45.-a, 05.45.Jn,84.30.-r

I. INTRODUCTION

Because of electromagnetic interference (which may be unintentional or intentional) [1], many circuits designed for low frequency operation may be subjected to radiofrequency (RF) signals. At high frequencies, the inductance in the wiring of these circuits combined with capacitance in semiconductor PN junctions can cause resonances, exposing the circuit to larger RF voltages than anticipated by the circuit designer. The large voltages, combined with the nonlinear voltage-dependant capacitances of the PN junctions, can cause nonlinear effects such as period doubling, chaos, and others. The simplest example of this type of effect is the diode resonator [2–10], which has been extensively studied.

There has been very little study of semiconductor circuits containing more than one PN junction. Period doubling and chaos have been observed in a transistor amplifier circuit [11], and in a microwave amplifier [12], but there has been no analysis and only very simple modeling of these effects in circuits more complicated than the diode resonator. There have been several chaotic oscillator circuits based on transistors [13–15], but those were self oscillatory circuits designed to be chaotic, while the present paper concerns a non-oscillatory circuit which is driven outside the range for which it was designed.

In this work, a single-transistor amplifier is studied experimentally and numerically. Not only are period doubling and chaos observed, but very low frequency switching between different complex waveforms is also seen. The low frequency behavior was seen both in the experiment and in a numerical model. This low frequency behavior could complicate the use of the amplifier when electromagnetic interference was present.

II. THE TRANSISTOR

The amplifier in the paper is based on a 2n929 transistor, a bipolar NPN transistor. Figure 1 is a simple block diagram of a transistor. The 3 terminals of the transistor are labeled base, collector and emitter. In this NPN transistor, the base is a layer of P-type

semiconductor material, while the collector and emitter are N-type, so that the transistor looks like two back-to-back PN junctions. The transistor is not the same as two back-to-back diodes because most of the current flowing from the collector or emitter into the base continues flowing through the base into the emitter or collector.

The resistors labeled R_{NC} or R_{NE} represent the nonlinear resistances of the PN junctions making up the transistor. In the simplest model, the resistors conduct no current until the voltage across them reaches some threshold, at which point the nonlinear resistance conducts current. The arrows on the nonlinear resistors indicate the direction of easy current flow. The actual behavior is more complicated. The functioning of the nonlinear resistances in the transistor may be described by the Ebers-Moll equations [16]. For an NPN transistor, such as the 2n929 used in the experiments above, the equations are

$$I_C = I_0 \left[- \left(e^{\frac{-qV_{CB}}{kT}} - 1 \right) + \alpha \left(e^{\frac{qV_{BE}}{kT}} - 1 \right) \right] \quad (1a)$$

$$I_E = I_0 \left[\left(e^{\frac{qV_{BE}}{kT}} - 1 \right) - \alpha \left(e^{\frac{-qV_{CB}}{kT}} - 1 \right) \right] \quad (1b)$$

$$I_B = I_C - I_E \quad (1c)$$

where I_C is the current flowing into the collector, I_B is the current flowing into the base, and I_E is the current flowing out of the emitter. V_{CB} is the collector-base voltage, V_{BE} is the base-emitter voltage, q is the charge of 1 electron, k is the Boltzmann constant, T is the temperature in Kelvins, and α is the fraction of current that flows from the collector, through the base, and into the emitter (or in the reverse direction). The fraction α is typically just below 1.0: for the 2n929 transistor, it was measured as 0.995.

Each PN junction also stores some charge, so the charge storage is represented by a capacitor in parallel with the nonlinear resistor. There are actually 2 types of charge storage in the PN junction [16], so C_C and C_E in Fig. 1 really stand for 2 capacitors in parallel. There is region at the actual junction between P and N type semiconductors that is depleted of charge, and this region acts like the dielectric in a parallel-plate capacitor. The charge

stored in this capacitor leads to the junction capacitance $C_J(V)$ (where V is the voltage across the PN junction) [17]

$$C_J(V) = \frac{C_J(0)}{\left((V - V_b)^2 + b\right)^{n/2}} \left(1 + \frac{n}{1 - n} \frac{b}{\left((V - V_b)^2 + b\right)}\right) \quad (2)$$

where V_b is the built-in voltage (approximately the turn on voltage) for the junction, V is the voltage across the junction, and b and n may be estimated by measuring junction capacitance as a function of V for $V < V_b$. Equation (2) is actually an approximation that is accurate only for $V < V_b$, but for $V > V_b$, the second type of capacitance described below dominates.

Outside of the depletion region, minority carriers diffuse into the bulk of the semiconductor, leading to the diffusion capacitance $C_D(V)$

$$C_D(V) = C_D(0) e^{\left(\frac{qV}{kT}\right)} \quad (3)$$

where q is the charge of 1 electron, k is the Boltzman constant, and T is the temperature in Kelvins.

In experiments with PN junctions (such as the diode resonator), the capacitance of the PN junction combines with stray inductance in the circuit wiring to form a series resonant circuit. Typical capacitances for PN junctions are on the order of 10^{-12} F or less (1 pF), so these resonances occur at frequencies of 1 GHz or greater. Acquiring data and building circuits at such high frequencies is difficult, so in the experiment described here, an inductor was added to the circuit to increase the inductance of the wiring, therefore lowering the resonant frequency to a range between 200 kHz and 30 MHz. In many of the plots in this paper, the frequency axis is normalized by this resonant frequency.

III. THE AMPLIFIER

Figure 2 is a schematic of the common-emitter amplifier used in the experiments. The transistor T_1 is a 2n929 bipolar transistor. The inductor L has been added to the amplifier

circuit to increase the inductance of the wiring so that the circuit behavior may be studied at lower frequencies. The output from the amplifier is the voltage V_L measured across the load resistor R_L . The values of the circuit components are given in the figure caption. Trim pots were used to create resistances that did not match standard resistance values.

The circuit was driven with a constant amplitude sine wave V_0 generated by a digital function generator. In order to further isolate the signal generator from the circuit, the signal V_0 was first passed through a broad-band preamplifier which acted as a buffer. To lessen the effect of the detection electronics on the amplifier circuit, a 100 k Ω resistor was placed between the location where V_L was measured and the detector.

IV. EXPERIMENT

As the frequency and amplitude of the driving signal V_0 were varied, period doubling and chaos were among the dynamical effects observed. Period doubling and chaos have been seen in other amplifier circuits [11,12] and in the diode resonator, so their presence was not surprising. What was surprising is that the DC level of V_L fluctuated slowly but periodically, oscillating at frequencies between 5 and 10 Hz. After passing through a 100 k Ω resistor, V_L was low-pass filtered through an amplifier which filtered out signals above 1000 Hz, and the filtered V_L signal was digitized. Figure 3 is a time series of the low-pass filtered output, which shows regular switching (the inductor L was set to 2200 μ H). Figure 4 shows the beginning and end of one of these switching events, with no low pass filtering.

The origin of this switching could be seen by digitizing the voltage V_C , which was the voltage at the collector of the transistor. An isolating probe was used to isolate the transistor circuit from the digital oscilloscope used to detect V_C . Two distinct states with different DC levels were observed for V_C . Figure 5(a) shows a plot of V_C vs. V_0 for the state corresponding to the higher DC level, while 5(b) is the state with the lower DC level. A slow but periodic switching between these 2 states was the cause of the low frequency switching seen in the amplifier output.

The frequency of this slow switching varied depending on the value of V_0 . Figure 6 is a plot of switching frequency as a function of the frequency and amplitude of V_0 , with black being the highest frequency and white corresponding to no switching. The frequency axis f_n is normalized by the resonant frequency of the series resonant circuit consisting of the inductor and the transistor. The base-emitter junction of the transistor acts as the capacitor in the series resonant circuit. The base-emitter capacitance, which varied as a function of bias voltage, was measured in the lab for the 2n929 transistor, and the capacitance at 0 bias, $C(0) = 24$ pF, was used to calculate the resonant frequency of the series LCR circuit. A frequency of $f_n = 1$ corresponds to the resonant frequency of this circuit, which for $L = 2200$ μH was approximately 693 kHz.

The switching frequency is quite sensitive to the parameters of the driving voltage, and there is a large region near the resonant frequency where no switching is seen. The bifurcation diagram in Fig. 7 shows why there is no switching in this region. The bifurcation diagram was created by plotting the value of V_C when the driving signal V_0 crossed 0 in the negative direction. The amplitude of V_0 for the bifurcation diagram was 5 V. The bifurcation diagram shows that low frequency switching exists only when attractors higher than period 1 exist. There is only 1 period 1 state, but there are at least two distinct types of waveform for states with periods higher than 1.

There was a lower driving frequency limit below which switching was not seen. Switching was observed for a resonant frequency of 459 kHz ($L = 5000$ μH), but not for a resonant frequency of 383 kHz ($L = 7200$ μH), although period doubling was seen for this resonant frequency. Low frequency switching was seen when the resonant frequency of the inductor-transistor combination was 10.2 MHz ($L = 10$ μH), but neither period doubling or low frequency switching was seen for a resonant frequency of 32 MHz ($L = 1$ μH). It has been shown in the diode resonator that period doubling for higher driving frequencies can be suppressed by the stray capacitance of the breadboard on which the circuit is assembled [2], so it is possible that low frequency switching could also exist at higher driving frequencies.

V. NUMERICAL SIMULATIONS

Numerical simulations are useful to confirm that the dynamical effects seen are indeed part of the transistor amplifier, and not caused by some other effect, such as an interaction with the driving signal source or the detection electronics. The simulations can also reveal if the model used for the transistor is adequate to produce the effects seen in the experiment.

The transistor may be described by eqs. (1-3), but the resulting model is difficult to work with. The exponential terms in eq. (1) and (3) make the resulting equations of motion stiff, requiring the use of a stiff numerical integration routine. Stiff routines are slower than integrators that are not stiff [18], and integration speed is a matter of concern in this problem. The amplifier circuit was driven at frequencies on the order of 1 MHz, while the switching events occurred at frequencies of a few Hz, so very long integration times will be necessary to model the switching. In order to make the simulations more practical, a simpler piecewise linear model for the transistor was substituted. A disadvantage of changing to the piecewise linear model is that there is no longer a direct correspondence between model parameters and the measurable physical parameters of the transistor.

The combined capacitances for the transistor were replaced with a single piecewise linear model. A similar model was used by Tanaka [8]. The capacitance model used here is

$$C_n(V, s) = \left\{ \begin{array}{ll} C_0 & |V| \leq V_{b1} \\ s(m_n V + b_n) & |V| > V_{b1} \end{array} \right\} \quad (4a)$$

$$b_n = s(C_0 - m_n V_{b1}) \quad (4b)$$

where V is the voltage across the junction, s is -1 for the collector-base junction and +1 for the base-emitter junction (the signs would be reversed for a PNP transistor), V_{b1} is 0.5 V, the 0 bias capacitance C_0 is 24 pF, and the slope $m_d = 500$ pF/V (the value of the slope was arbitrary).

The nonlinear current equations (eq. 1) were also replaced with

$$I_C = I_0 [g_n(V_{CB}, -1) + \alpha g_n(V_{BE}, 1)] \quad (5a)$$

$$I_E = I_0 [g_n (V_{BE}, 1) + \alpha g_n (V_{CB}, -1)] \quad (5b)$$

$$I_B = I_C - I_E \quad (5c)$$

$$g_n (V, s) = \left\{ \begin{array}{ll} 0 & |V| \leq V_{b2} \\ m_I V + b_I & |sV| > V_{b2} \end{array} \right\} \quad (5d)$$

$$b_I = s m_I V_{b2} \quad (5e)$$

where the slope $m_1 = 10^{-4}$ A/V , and the turn-on voltage V_{b2} was 0.6 V. The break point voltage in the capacitance function of eq. (4) (V_{b1}) was slightly less than the turn-on voltage V_{b2} because the capacitance value starts to rise before the transistor turns on.

The slope constant m_1 in eq. (5) was set by simulating the characteristic curves for the transistor, where the collector current I_C is plotted as a function of the collector-emitter voltage V_{CE} for different levels of the base current I_b [19]. Figure 8 shows a characteristic curve plot for the 2n929 transistor (measured experimentally), where the base current values for the curves were $0.5 \mu\text{A}$, $1.7 \mu\text{A}$, $2.9 \mu\text{A}$, $4.1 \mu\text{A}$, and $5.3 \mu\text{A}$. Figure 9 shows the characteristic curves from the piecewise linear simulation, with base current values of $0.19 \mu\text{A}$, $0.67 \mu\text{A}$, $1.1 \mu\text{A}$, $1.6 \mu\text{A}$ and $2.1 \mu\text{A}$. These plots are a standard method for characterizing a transistor. The simulated curves were compared with actual curves, and m_1 was chosen to make the simulations roughly match the experimental curves. The full equations of motion for the transistor amplifier were

$$\frac{dx_1}{dt} = - \left(\frac{J_1 + I_C R_c R_l}{R_c R_l C_n(x_1, -1)} \right) \quad (6a)$$

$$\frac{dx_2}{dt} = - \left(\frac{J_4 R_1 + J_5 R_2 + I_e R_c R_l R_A}{R_c R_l R_A C_n(x_2, 1)} \right) \quad (6b)$$

$$\frac{dx_3}{dt} = \frac{- \left(\frac{R_1 (R_b V_a + R_2 R_b x_3 + R_2 x_4)}{R_1 R_2 + R_1 R_b + R_2 R_b} \right) + x_5}{L} \quad (6c)$$

$$\frac{dx_4}{dt} = \frac{I_e + \frac{x_2}{R_e} - \frac{x_4}{R_e} - \frac{(J_4 R_1 + J_5 R_2 + I_e R_c R_l R_A)(C_6 + C_n(x_2, 1))}{R_c R_l R_A C_n(x_2, 1)}}{C_6} \quad (6d)$$

$$\frac{dx_5}{dt} = \frac{dV_0}{dt} - \frac{x_3}{C_1} \quad (6e)$$

$$\begin{aligned} \frac{dx_6}{dt} = & \frac{I_e R_e + x_2 - x_4}{C_6 R_e} - \frac{x_6}{C_l R_l} - \frac{J_1 + I_C R_c R_l}{R_c R_l C_n(x_1, -1)} \\ & - \frac{(J_4 R_1 + J_5 R_2 + I_e R_c R_l R_A) (C_6 + C_n(x_2, 1))}{C_6 R_c R_l R_A C_n(x_2, 1)} \end{aligned} \quad (6f)$$

$$R_A = (R_2 R_b + R_1 (R_2 + R_b)) \quad (6g)$$

$$J_1 = (R_l (-V_a + x_1 + x_4) + R_c x_6) \quad (6h)$$

$$J_2 = (R_l (V_1 - R_c x_3) + R_c x_6) \quad (6i)$$

$$J_3 = (J_2 + J_1 R_b + R_c R_l (-V_a + x_4)) \quad (6j)$$

$$J_4 = (J_2 R_2 + J_1 R_b + R_c R_l (-V_a + x_4)) \quad (6k)$$

$$J_5 = (J_1 R_b + R_c R_l x_4) \quad (6l)$$

V_a is the power supply voltage of +15 V. The variable x_1 corresponds to the collector-base voltage, x_2 corresponds to the base-emitter voltage, x_3 is the current through the inductor L , x_4 is the voltage at the base of the transistor, x_6 is the voltage at the junction of the input capacitor C_1 and the inductor L , and x_6 is the voltage across the load resistor R_L . Voltages other than x_1 and x_2 were referenced to ground. R_b is added to the model to simulate the base resistance of approximately 50 Ω , and the inductor L was set to 2000 μH , while all other component values are the same as in the circuit. The terms R_A and J_1 through J_5 do not have any particular units, but are added to make it possible to write the equations on one page.

The large separation in time scales between the driving frequency and the response frequency of the transistor amplifier made it impractical to do extensive parameter variation

studies, so the model was used only to verify that the low frequency switching was indeed possible in the transistor amplifier circuit by itself, and not caused by some other artifact of the experiment.

In the experiment, it was observed that varying the values of the capacitors C_1 , C_2 and C_3 by a factor of 10 did not affect the driving frequencies or amplitudes at which low frequency switching was seen, nor was the distribution of switching frequencies affected. Since the results of the experiment weren't very sensitive to the values of these capacitors, for the simulation they were all set to $1 \mu\text{F}$ in order to reduce the length of the initial transient in the simulations.

The simulations of equation 6 used a 4'th order Runge-Kutta integration routine [18] with a stepsize of 10^{-8} s. Each simulation was first run for 20,000,000 steps to eliminate the long initial transient. Figure 10 is a bifurcation plot from eq. (6), where f_n is the driving frequency divided by the inductor-transistor resonant frequency of 795 kHz, and x_1 is the value of x_1 when the driving signal crosses 0 in the positive direction. The driving amplitude for Fig. 10 was 15 V. Signal amplitudes in the piecewise linear model do not correspond directly to signal amplitudes in the actual amplifier. The bifurcation plot does show regions of complex behavior, but unlike the experiment, all of this behavior occurs only for frequencies below the resonant frequency. Figure 11 shows a time series of the value of x_1 at the positive-going zero crossings of the driving signal, for a driving frequency of 500 kHz ($f_n = 0.63$). Low frequency switching between two different types of behavior is clearly seen. The switching frequency is 115 Hz. Figure 12 shows Poincare sections from the two different types of oscillation. Figure 12(a) is a Poincare section of x_2 vs. x_1 for the larger oscillation, while (b) is a Poincare section for the smaller oscillation. As in the experiment, different waveforms are present during the two different types of oscillation.

VI. CONCLUSIONS

This paper has shown that driving a transistor amplifier with a high frequency signal can cause very low frequency switching. The low frequency switching was seen in an experiment, and its existence was confirmed in a simple piecewise linear model of the transistor amplifier.

No such switching has been reported in the well-studied diode resonator circuit, which has only a single PN junction, so it is almost certain that the double PN junction in the transistor is responsible for the switching. This switching was not observed in my lab in a back-to-back pair of diodes, but because of the narrow base layer of the transistor, it is not the same as a simple pair of diodes.

Low frequency switching was seen in other types of transistors besides the one reported here, including a MOSFET power transistor.

This paper does not address the cause of the low frequency switching. The large frequency difference between the driving signal and the switching means that specialized mathematical techniques for analyzing fast-slow systems must be employed. It is anticipated that further analysis will be undertaken in the future.

REFERENCES

- [1] V. I. Ponomarenko, M. D. Prokhorov and Y. P. Seleznev, *Low-dimensional model of a microwave resonator with a p-n junction varactor*, IEEE-Russia Conference on High Power Microwave Electronics: Measurements, Identification, Applications., 1999, (IEEE)
- [2] T. L. Carroll and L. M. Pecora, *Physical Review E* **66**, 046219 (2002)
- [3] E. R. Hunt and R. W. Rollins, *Physical Review A* **29**, 1000-1002 (1984)
- [4] C. M. Kim, C. H. Cho and C. S. Lee, *Physical Review A* **38**, 1645-1648 (1988)
- [5] P. S. Linsay, *Physical Review Letters* **47**, 1349-1352 (1981)
- [6] Z. Su, R. W. Rollins and E. R. Hunt, *Physical Review A* **40**, 2698-2705 (1989)
- [7] N. Takeuchi, T. Nagai and T. Matsumoto, *Electronics and Communications in Japan* **84**, 91-99 (2001)
- [8] S. Tanaka, S. Higuchi and T. Matsumoto, *Physical Review E* **54**, 6014-6028 (1996)
- [9] J. Testa, J. Perez and C. Jeffries, *Physical Review Letters* **48**, 714-717 (1982)
- [10] R. M. d. Morales and S. Anlage, submitted to *IEEE Transactions on Circuits and Systems Part I* (2002)
- [11] D. J. Jeffries, G. G. Johnstone and J. H. B. Deane, *International Journal of Electronics* **71**, 661-673 (1991)
- [12] P. Perry, P. O'Halloran and T. J. Brazil, *Observation of chaos in a 2.4 GHz amplifier*, 3rd International Specialist Workshop on Nonlinear Dynamics of Electronic Systems (NDES '95), 1995, (IEEE)
- [13] M. P. Kennedy, *IEEE Transactions on Circuits and Systems Part I*, **41**, 771 (1994)
- [14] A. Tamasevicius, G. Mykolaitis, S. Bumeliene, A. Cenys, A. N. Anagnostopoulos, and

- E. Lindberg, *Electronics Letters* **37**, 549 (2001)
- [15] N. F. Rulkov and A. R. Volkovskii, *IEEE Transactions on Circuits and Systems Part I* **48**, 673 (2001)
- [16] M. J. Cooke, *Semiconductor Devices* (Prentice Hall, Englewood Cliffs, 1990)
- [17] H. C. Poon and H. K. Gummel, *Proceedings of the IEEE* **57**, 2181-2182 (1969)
- [18] W. H. Press, B. P. Flannery, S. A. Teukolsky and W. T. Vetterling, *Numerical Recipes* (Cambridge University Press, New York, 1990)
- [19] U. Tietze and C. Shenk, *Electronic Circuits* (Springer, Berlin, 1991)

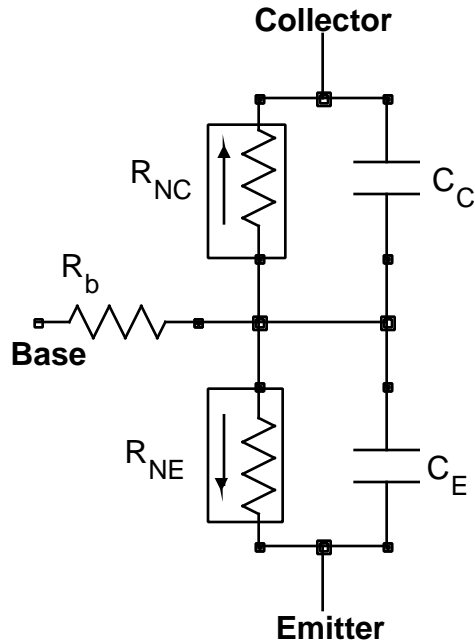


Figure 1. Block diagram of an NPN transistor. R_b represents the base resistance of approximately 50Ω , while R_{NC} and R_{NE} represent the nonlinear resistances of the transistor. C_C and C_E represent the capacitances of the transistor.

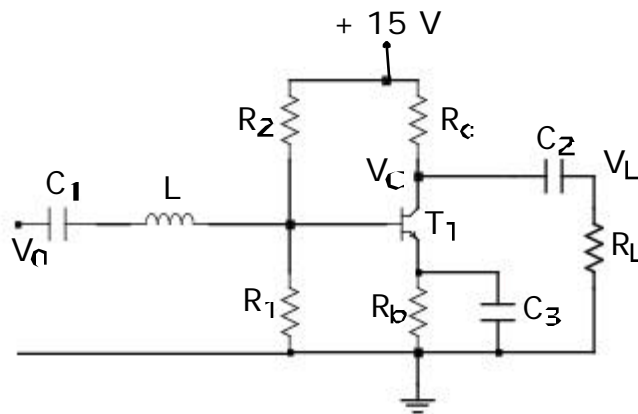


Figure 2. Schematic of the amplifier circuit used in the experiments. The component values are $R_1 = 40,420 \Omega$, $R_2 = 204545 \Omega$, $R_c = 15,000 \Omega$, $R_e = 3750 \Omega$, $R_L = 1 \text{ M}\Omega$, $C_1 = C_2 = 25 \mu\text{F}$, $C_3 = 330 \mu\text{F}$, $L = 2200 \mu\text{H}$, and the transistor T_1 is of type 2n929. The driving voltage is applied at the location marked V_0 , and the output voltage is measured at V_L .

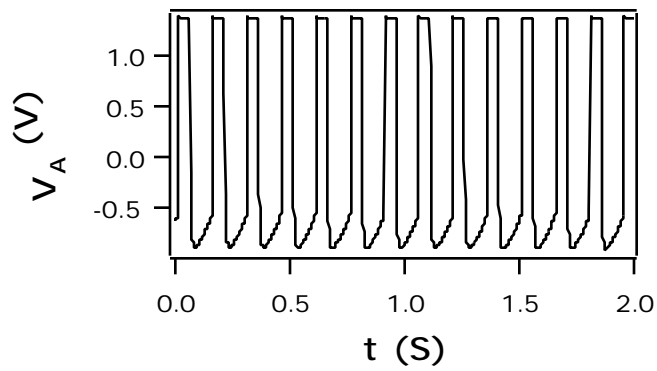


Figure 3. Low-pass filtered signal V_L when low frequency switching is present. The low pass filter break frequency was 1 kHz.

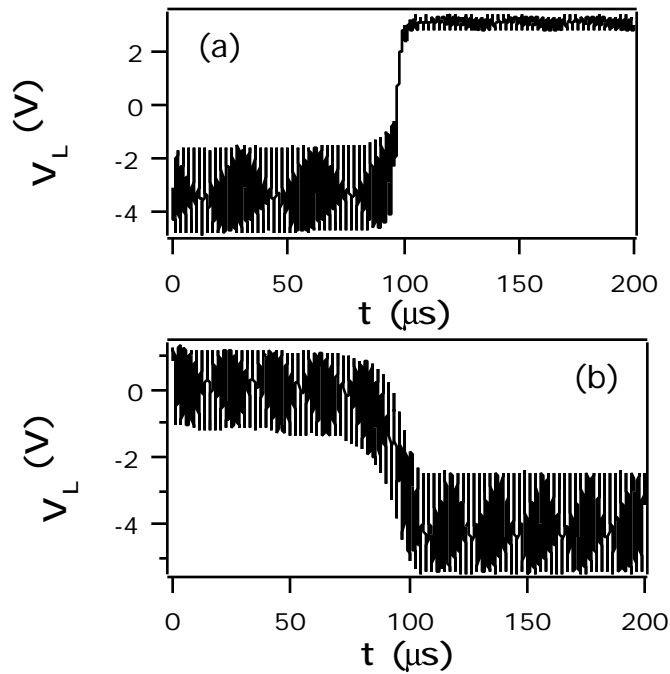


Figure 4(a) Unfiltered V_L signal at the start of a switching event. (b) Unfiltered V_L at the end of a different switching event. The time scale of a complete switching event was on the order of 0.1 s.

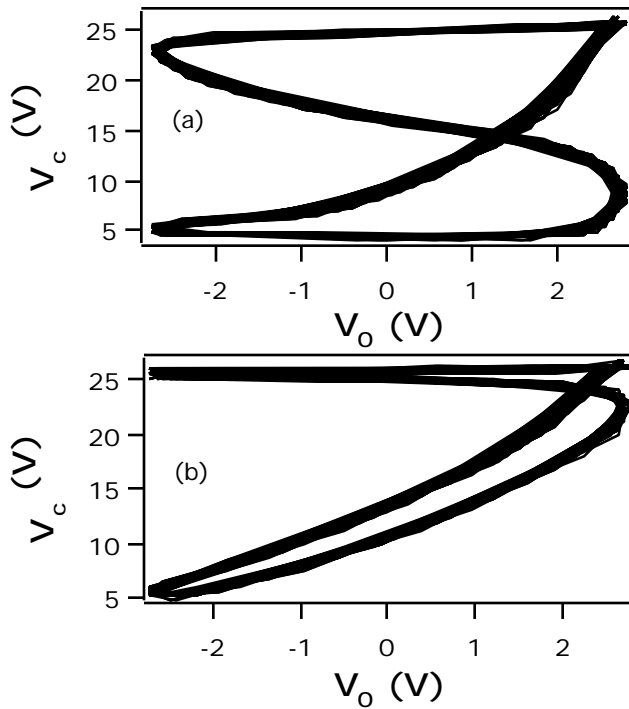


Figure 5. Phase space plots of V_C , the voltage at the collector, vs the driving voltage V_O during the two different parts of a switching event. The two V_C waveforms have different DC components, leading to the large DC swings seen in Fig. 3.

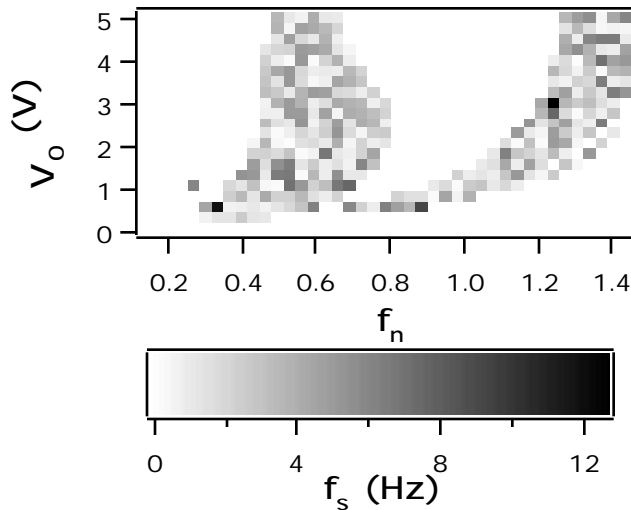


Figure 6. Frequency of the slow switching for different amplitudes and frequencies of the driving signal, where black is the highest value and white corresponds to zero. f_n is the driving frequency normalized by the resonant frequency of the inductor-transistor series resonant circuit. The lower graph gives the frequency scale for the upper graph, where f_s is the switching frequency.

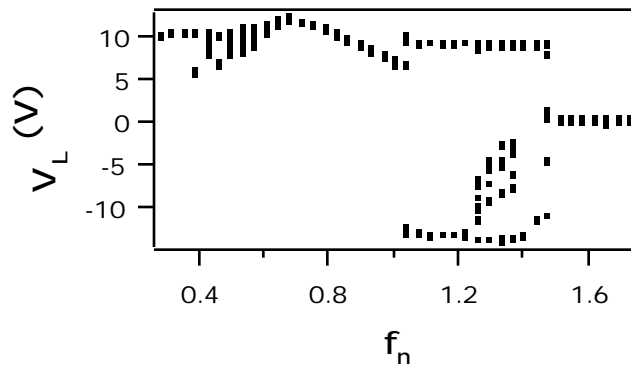


Figure 7. Bifurcation plot of V_L from the transistor amplifier experiment strobed when the driving signal V_0 crosses 0 in the positive direction. f_n is the driving frequency normalized by the resonant frequency of the inductor-transistor series resonant circuit. The amplitude of the driving signal was 5 V. The regions where period 2 or higher behavior was seen in the bifurcation plot coincide with the regions where slow switching was seen.

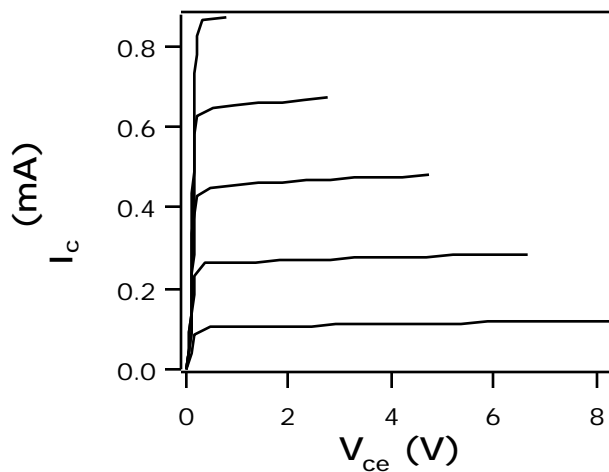


Figure 8. Characteristic curves of the collector current I_C vs. the collector-emitter voltage V_{CE} at different base currents for the 2N929 bipolar transistor used in the circuit of Fig. 1. The base currents for these curves (starting at the bottom) were $0.5 \mu\text{A}$, $1.7 \mu\text{A}$, $2.9 \mu\text{A}$, $4.1 \mu\text{A}$, and $5.3 \mu\text{A}$.

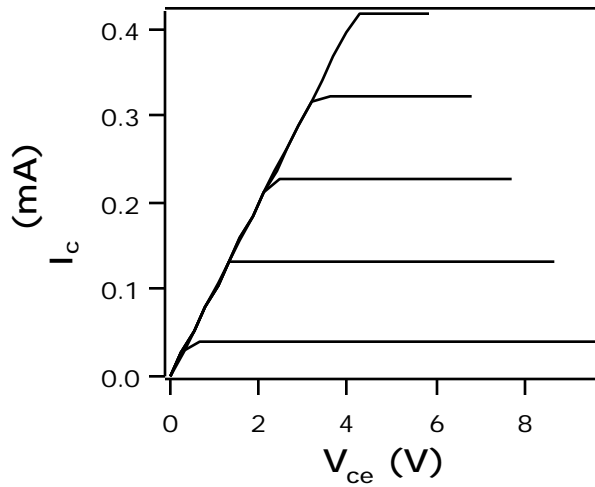


Figure 9. Characteristic curves of the collector current I_C vs. the collector-emitter voltage V_{CE} at different base currents for the piecewise linear model of a transistor amplifier. The base currents for these curves (starting at the bottom) were $0.19 \mu\text{A}$, $0.67 \mu\text{A}$, $1.1 \mu\text{A}$, $1.6 \mu\text{A}$, and $2.1 \mu\text{A}$.

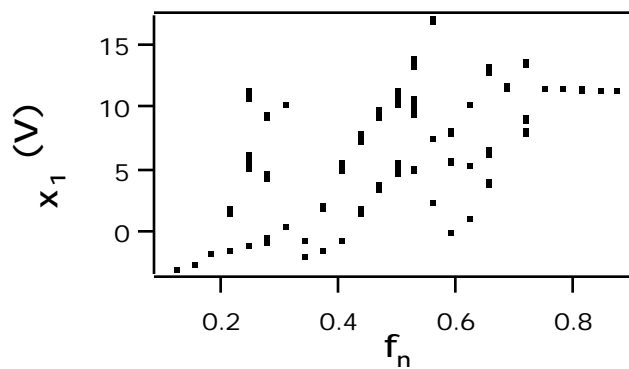


Figure 10. Bifurcation plot from the model of eq. (6), with a driving amplitude of 15 V. f_n is the driving frequency normalized by the resonant frequency of the inductor-transistor series resonant circuit. The x_1 signal was strobed on the positive-going zero crossing of the driving signal.

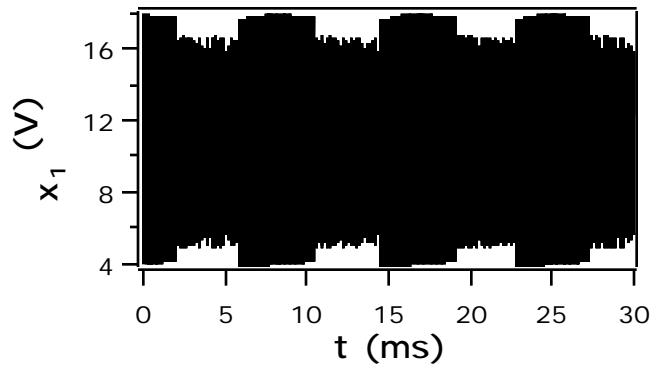


Figure 11. Time series of the strobed x_1 signal from the model of eq. (6), when the driving amplitude was 15 V and the driving frequency was 500 kHz ($f_n = 0.63$). The frequency of the large switching events is 115 Hz.

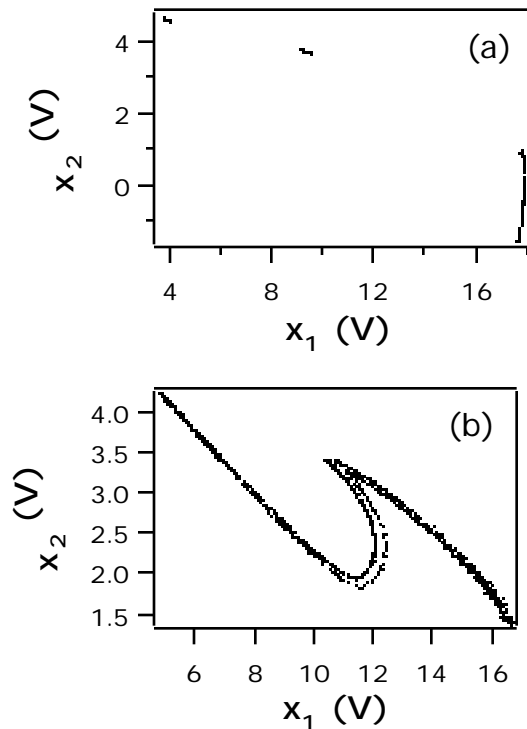


Figure 12. Poincaré sections of 2 signals from the model of eq. (6) (strobed at the positive-going zero crossing of the drive signal) for a drive amplitude of 15 V and frequency of 500 kHz. (a) is for the larger oscillation in Fig. 11, while (b) is for the smaller oscillation.